

Significance of the Molecular Shape of Iron Corrphycene in a Protein Pocket

Saburo Neya,^{*†} Kiyohiro Imai,[‡] Yoshitsugu Hiramatsu,[§] Teizo Kitagawa,[§] Tyuji Hoshino,[†] Masayuki Hata,[†] and Noriaki Funasaki^{||}

Department of Physical Chemistry, Graduate School of Pharmaceutical Sciences, Chiba University, Inage-Yayoi, Chiba 263-8522, Japan, Department of Material Chemistry, Faculty of Engineering, Hosei University, Koganei, Tokyo 184-8584, Japan, Center for Integrative Bioscience, Okazaki National Institutes, Okazaki, Aichi 444-8787, Japan, and Department of Physical Chemistry, Kyoto Pharmaceutical University, Yamashina, Kyoto 607-8414, Japan

Received January 13, 2006

The iron complex of a new type of corrphycene bearing two ethoxycarbonyl ($-\text{CO}_2\text{C}_2\text{H}_5$) groups on the bipyrrole moiety was introduced into apomyoglobin. The reconstituted ferric myoglobin has a coordinating water molecule that deprotonates to hydroxide with a $\text{p}K_{\text{a}}$ value of 7.3 and exhibits 3–10-fold higher affinities for anionic ligands when compared with a counterpart myoglobin with the same substituents on the dipyrroethene moiety. In the ferrous state, the oxygen affinity of the new myoglobin was decreased to $1/410$ of the native protein. The anomalies in the ligand binding, notably dependent on the side-chain location, were interpreted in terms of a characteristic core shape of corrphycene that produces the longer and shorter Fe–N(pyrrole) bonds. The spin-state equilibrium analysis of the ferric azide myoglobin containing the new iron corrphycene supported the nonequivalence of the Fe–N(pyrrole) bonds. These results demonstrate that the trapezoidal molecular shape of corrphycene exerts functional significance when the iron complex is placed in a protein pocket.

Introduction

The integrated molecular structure of porphyrin is the essential determinant of the reactivity of a coordinating metal ion. Recent advances in porphyrin synthesis created novel porphyrin isomers with variously arranged tetrapyrrole alignment.¹ Vogel and co-workers in 1986 discovered the first porphyrin isomer, porphycene, and demonstrated that the tetrapyrrole rearrangement dramatically alters the physical properties of the parent porphyrin.² Corrphycene is the second isomeric porphyrin found out in 1994 independently by Sessler et al.³ and by Aukauloo and Guilard.⁴ Apomyo-

globin (apoMb) has been employed as a matrix for an unnatural prosthetic group and to bring out the biological activity of these and other porphyrinoids. The reconstituted Mb's containing the iron complexes of oxochlorins,⁵ etio-corrphycene,⁶ porphycene,^{7,8} azaporphyrins,^{9,10} and hemiporphycene¹¹ are known to exhibit very characteristic spectroscopic and ligand-binding profiles.

Corrphycene has a trapezoidal molecular shape, and the constituting pyrroles are classified into the bipyrrole and dipyrroethene groups. Owing to the unique structure, when

* To whom correspondence should be addressed. E-mail: sneya@p.chiba-u.ac.jp.

† Chiba University.

‡ Hosei University.

§ Okazaki National Institutes.

|| Kyoto Pharmaceutical University.

- (1) Sessler, S. L.; Gebauer, A.; Vogel, E. In *The Porphyrin Handbook*; Kadish, K. M., Smith, K. M., Guilard, R., Eds.; Academic Press: San Diego, CA, 2000; Vol. 2, pp 1–54.
- (2) Vogel, E.; Köcher, M.; Schmickler, H.; Lax, J. *Angew. Chem., Int. Ed. Engl.* **1986**, *25*, 257–259.
- (3) Sessler, J. L.; Brucker, E. A.; Weghorn, S. J.; Kisters, M.; Schäfer, M.; Lex, J.; Vogel, E. *Angew. Chem., Int. Ed. Engl.* **1994**, *33*, 2308–2312.
- (4) Aukauloo, M. A.; Guilard, R. *New J. Chem.* **1994**, *18*, 1205–1207.

- (5) Sotiriou-Leventis, C.; Chang, C. K. *Inorg. Chim. Acta* **2000**, *311*, 113–118.
- (6) Neya, S.; Nakamura, M.; Imai, K.; Funasaki, N. *Chem. Pharm. Bull.* **2001**, *49*, 345–346.
- (7) Hayashi, T.; Dejima, H.; Matsuo, T.; Sato, H.; Murata, D.; Hisaeda, Y. *J. Am. Chem. Soc.* **2002**, *124*, 11226–11227.
- (8) Mastuo, T.; Dejima, H.; Hirota, S.; Murata, D.; Sato, H.; Ikegami, T.; Hori, H.; Hisaeda, Y.; Hayashi, T. *J. Am. Chem. Soc.* **2004**, *126*, 16007–16017.
- (9) Neya, S.; Kaku, T.; Funasaki, N.; Shiro, Y.; Iizuka, T.; Imai, K.; Hori, H. *J. Biol. Chem.* **1995**, *270*, 13118–13123.
- (10) Neya, S.; Hori, H.; Imai, K.; Kawamura-Konishi, Y.; Suzuki, H.; Shiro, Y.; Iizuka, T.; Funasaki, N. *J. Biochem.* **1997**, *121*, 645–660.
- (11) Neya, S.; Imai, K.; Hori, H.; Ishikawa, H.; Ishimori, K.; Okuno, D.; Nagatomo, S.; Hoshino, H.; Hata, M.; Funasaki, N. *Inorg. Chem.* **2003**, *42*, 1456–1461.

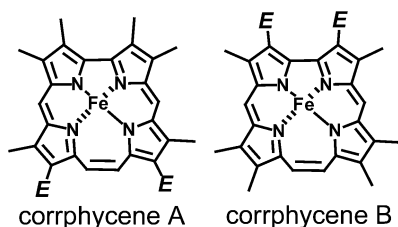


Figure 1. Structure of the iron corrphycenes. E stands for ethoxycarbonyl group $-\text{CO}_2\text{C}_2\text{H}_5$.

corrphycene is peripherally substituted with functional groups, the substituent effect is expected to be different between the bipyrrrole and dipyrroethene units. It will be of primary interest to follow up the significance of the peculiar molecular shape of corrphycene.

We have previously prepared 2,3,6,7,11,18-hexamethyl-12,17-bis(ethoxycarbonyl)corrphycene (corrphycene A; Figure 1)¹² and reported that the ethoxycarbonyl ($-\text{CO}_2\text{C}_2\text{H}_5$) groups attached to the dipyrroethene moiety considerably alter the functional and physical properties of Mb.^{13,14} In pursuit of the underlying significance of the characteristic molecular shape, we synthesized a new derivative, 2,7,11,12,17,18-hexamethyl-3,6-bis(ethoxycarbonyl)corrphycene (corrphycene B; Figure 1), where the ester groups are migrated to the bipyrrrole unit. Corrphycene A and B provide a unique opportunity to analyze the side-chain effect in the trapezoidal tetrapyrrole. We addressed the following questions about corrphycene. Is there any appreciable difference between the iron complexes of corrphycene A and B? If it were so, how much is the extent and how does the difference arise? What is the functional consequence in a protein matrix? To solve these issues, we characterized the Mb-containing iron corrphycene B (Mb-B) and compared the results with the counterpart Mb-bearing iron corrphycene A (Mb-A).^{13,14} The results reveal a significance of the trapezoidal molecular shape of iron corrphycene in globin.

Materials and Methods

Synthesis of Corrphycene B. 3,3',4,4'-Tetramethyl-2,2'-dipyrroethane-5,5'-dicarboxylic acid¹⁵ (120 mg) was dissolved in 5 mL of trifluoroacetic acid, and the solution was stirred for 30 min at room temperature. After the addition of ethyl 2-formyl-3-methylpyrrole-5-carboxylate¹⁶ (143 mg) and 30% hydrogen bromide in acetic acid (2 mL) to the trifluoroacetic acid solution, the mixture was stirred for a further 60 min and cooled on ice. The resultant *a,c*-biladine-like linear tetrapyrrole was collected after filtration (167 mg, 60% yield). ¹H NMR (400 MHz, CDCl_3 , δ): 13.57, 13.48 (each br s, 2H, NH), 8.12 (m, 2H, ring H), 7.35 (s, 2H, $=\text{CH}-$), 4.30 (q, 4H, $-\text{CH}_2\text{CH}_3$), 3.58 (s, 4H, $-\text{CH}_2\text{CH}_2-$), 3.49, 2.63, 2.35 (each s, 6H, ring $-\text{CH}_3$), 1.36 (t, 6H, $-\text{CH}_2\text{CH}_3$). Corrphycene B was synthesized by the copper(II)-promoted cyclization as we reported

for corrphycene A.¹² The dimethylformamide (DMF) containing the above linear tetrapyrrole (500 mg) and $\text{CuCl}_2 \cdot 2\text{H}_2\text{O}$ (1.0 g) was refluxed over 60 min to facilitate cyclization to the copper chelate. The copper complex was purified on a silica gel column with 100:3 chloroform/methanol and demetalated with sulfuric acid to afford the free base of corrphycene B (75 mg, 20% from the tetrapyrrole). ¹H NMR (400 MHz, CDCl_3 , δ): 9.76 (s, 2H, $-\text{CH}=\text{CH}-$), 9.55 (s, 2H, $-\text{CH}=\text{CH}-$), 4.67 (q, 4H, $-\text{CH}_2\text{CH}_3$), 3.63, 3.37, 3.35 (each s, 6H, ring $-\text{CH}_3$), 1.50 (t, 6H, $-\text{CH}_2\text{CH}_3$), -0.42 (br s, 2H, NH). Anal. Calcd for $\text{C}_{32}\text{H}_{34}\text{N}_4\text{O}_4$: C, 71.35; H, 6.36; N, 10.54. Found: C, 71.04; H, 6.67; N, 10.33. MS: *m/z* 539 ($M + 1$). UV/visible [dichloromethane; λ_{max} , nm (ϵ , $\text{M}^{-1} \text{cm}^{-1}$): 416 (98 000), 518 (7090), 554 (7940), 583 (3520), 636 (4740). The ferric iron chloride complex prepared after Adler et al.¹⁷ was purified on a silica gel column with 100:3 chloroform/methanol.

Mb Reconstitution. Sperm whale Mb (type II) was available from Sigma. The Mb reconstitution with iron corrphycene B was carried out as described for the isomer A.¹⁴ The crude protein was purified on a (carboxymethyl)cellulose (Whatman CM 52) column.¹⁴ The purified ferric Mb-B was determined at 421 nm with $\epsilon = 93 \text{ mM}^{-1} \text{cm}^{-1}$, which is based on $\epsilon = 18 \text{ mM}^{-1} \text{cm}^{-1}$ at 575 nm for the ferrous hemochromogen complex¹⁸ in 1:1 pyridine/DMF.

Ligand Binding. The anionic ligands were commercially available and used as received. The ligand-binding constant of ferric Mb was determined by the spectrophotometric titration. The oxygen equilibrium curve of ferrous Mb was measured on the automatic recording apparatus of Imai.¹⁹

Physical Measurements. UV/visible and IR absorption spectra were recorded on a Shimadzu MPS-2000 and a Nicolet Avatar spectrometer, respectively.

Results

Macrocycle. Our initial forecast on the formation of corrphycene B was negative because the precursory linear tetrapyrrole may be unreactive owing to the moderately bulky and deactivating ethoxycarbonyl groups on the terminal pyrroles. Fortunately, the copper(II)-mediated cyclization⁵ was successful to afford the copper chelate in 20% yield. The visible absorption spectra of corrphycene A and B are compared in Figure 2. The Soret band of the free base of corrphycene B is at 416 nm, identical with that of the isomer A. However, the peak intensity ($\epsilon = 98 \text{ mM}^{-1} \text{cm}^{-1}$) is slightly lower than $102 \text{ mM}^{-1} \text{cm}^{-1}$ of corrphycene A. The visible absorption of corrphycene B is not of the etio-type observed in the A isomer. The pK_3 value of the corrphycene B free base, as determined with the reported method in 2.5% aqueous sodium dodecyl sulfate,²⁰ was 2.4 ± 0.2 (result not shown). The value is identical with that reported for corrphycene A.⁷

Reconstituted Mb and Ligand Binding. Spectrophotometric titration of apoMb with ferric corrphycene B indicated a clear inflection point at a 1:1 stoichiometry. The reconstituted Mb-B was stable at room temperature. Figure 3

(12) Neya, S.; Nishinaga, K.; Ohshima, K.; Funasaki, N. *Tetrahedron Lett.* **1998**, *39*, 5217–5220.

(13) Neya, S.; Funasaki, N.; Hori, H.; Imai, K.; Nagatomo, S.; Iwase, T.; Yonetani, T. *Chem. Lett.* **1999**, *28*, 989–990.

(14) Neya, S.; Tsubaki, M.; Hori, H.; Yonetani, T.; Funasaki, N. *Inorg. Chem.* **2001**, *40*, 1220–1225.

(15) Vogel, E.; Bröring, M.; Fink, J.; Rosen, D.; Schmickler, H.; Lex, J.; Chan, K. W. K.; Wu, Y.-D.; Plattner, D. A.; Nendel, M.; Houk, K. *Angew. Chem., Int. Ed. Engl.* **1995**, *24*, 2511–2514.

(16) Paine, J. B.; Dolphin, D. *J. Org. Chem.* **1988**, *53*, 2787–2795.

(17) Adler, A. D.; Longo, F.; Kampas, F.; Kim, J. J. *Inorg. Nucl. Chem.* **1970**, *32*, 2443–2445.

(18) Antonini, E.; Brunori, M. *Hemoglobin and Myoglobin in their Reactions with Ligands*; North-Holland: Amsterdam, The Netherlands, 1971; pp 47 and 48.

(19) Imai, K. *Methods Enzymol.* **1981**, *76*, 438–449.

(20) Smith, K. M. In *Porphyrin and Metalloporphyrins, a New Edition Based on the Original Volume by J. E. Falk*; Smith, K. M., Ed.; Elsevier: Amsterdam, The Netherlands, 1975; pp 11–14.

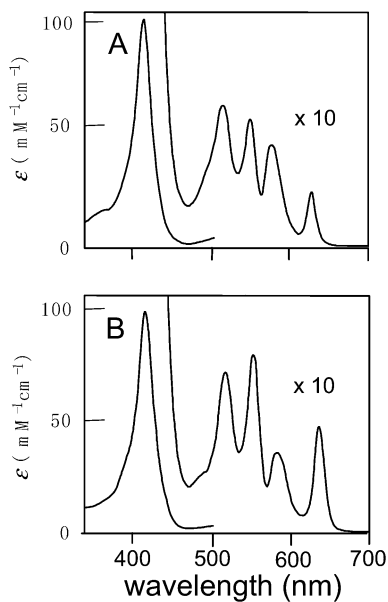


Figure 2. Electronic absorption spectra of the free bases in dichloromethane: (A) corrphycene A; (B) corrphycene B.

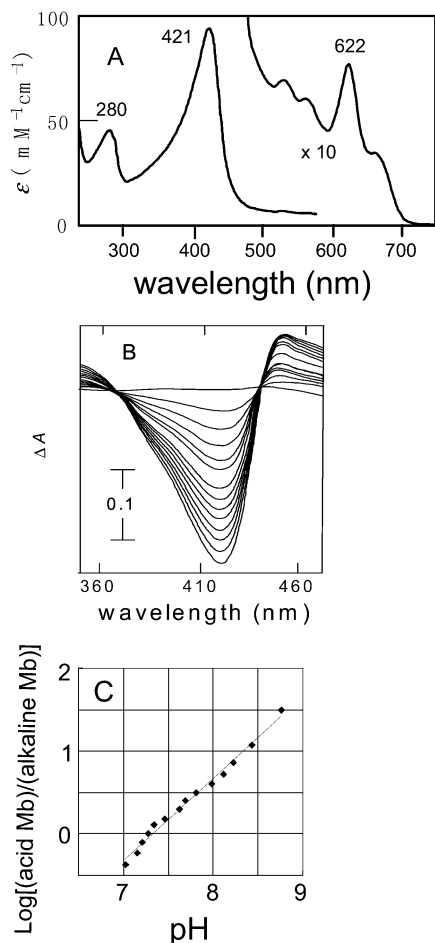


Figure 3. Ferric aquamet Mb-B: (A) electronic absorption spectrum in 0.1 M Tris at pH 7.0 and 20 °C; (B) Soret absorption changes of ferric aquamet Mb-B in 10 mM Tris at 20 °C over pH 7.02–8.76; (C) analysis of the changes in part B at 412 nm. The slope is 0.99, and the midpoint of the transition is at pH 7.33 ± 0.18 .

shows the electronic absorption spectrum of the ferric Mb-B, where the Soret band is 2.1-fold higher than the 280-nm

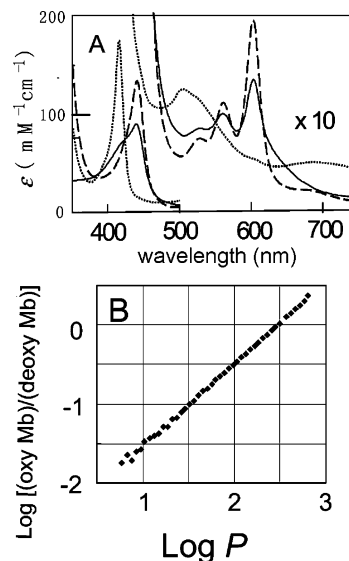


Figure 4. Ferrous Mb-B. (A) Visible absorption spectra of the oxy (solid curve), deoxy (broken curve), and carbon monoxy (dotted curve) derivatives of 0.1 M phosphate at pH 7.4 and 20 °C. Owing to the low affinity, O₂ saturation of the “oxyMb” is only ~34% under 1 atm of air. (B) O₂ equilibrium curve in 0.1 M phosphate at pH 7.4 and 20 °C. The Hill coefficient is $n = 1.04$, and the partial oxygen pressure at half-saturation is $P_{50} = 300$ mmHg. Monitored at 605 nm.

globin peak. The peak intensity was notably pH-dependent, and the analysis of the transition over pH 7–9 afforded a midpoint at pH 7.33 (Figure 3). Exogenous ligands such as N₃⁻, OCN⁻, SCN⁻, F⁻, and imidazole bound with affinities of $(9.36 \pm 0.21) \times 10^4$, $(1.74 \pm 0.10) \times 10^4$, $(1.86 \pm 0.09) \times 10^4$, $(3.37 \pm 0.21) \times 10^4$, 337 ± 18 , and 198 ± 14 M⁻¹, respectively, in a 0.1 M Tris buffer at pH 7.0 and 20 °C. The high affinity of CN⁻, $(1.34 \pm 0.12) \times 10^6$ M⁻¹, was estimated with the method of Brown.²¹ The reduced protein is functionally active to bind O₂ and CO reversibly, as indicated in Figure 4. Figure 4 also displays the oxygen equilibrium curve of Mb-B. The Hill coefficient $n = 1.04$ and the oxygen pressure at a half-saturation of 300 mmHg were obtained. The oxygen affinity is much lower than $P_{50} = 0.73$ mmHg of the native Mb.²² Table 1 compiles the visible absorption spectra of the ferric and ferrous derivatives.

Spin Equilibrium. The azide hemoprotein is in an equilibrium between the high- ($S = 5/2$) and low-spin ($S = 1/2$) states. The equilibrium is sensitive to the electronic perturbation to the iron porphyrins.^{14,23–26} We monitored the equilibrium in the azide complex of ferric Mb-B to characterize further corrphycene B in protein. Figure 5 shows the IR spectra of the iron-bound azide (N₃⁻) in Mb-B and the model compounds, where the major and minor bands were identified at 2046 and 2022 cm⁻¹ for Mb-B and at 2048 and 2019 cm⁻¹ for the six-coordinate N₃⁻/1-methylimidazole model. These peaks are clearly different in position from

(21) Brown, K. L. *Inorg. Chim. Acta* **1979**, L513–L516.

(22) Sono, M.; Asakura, T. *J. Biol. Chem.* **1975**, *250*, 5227–5232.

(23) McCoy, S.; Caughey, W. S. *Biochemistry* **1970**, *9*, 2387–2393.

(24) Neya, S.; Chang, C. K.; Okuno, D.; Hoshino, T.; Hata, M.; Funasaki, N. *Inorg. Chem.* **2005**, *44*, 1193–1195.

(25) Neya, S.; Hada, S.; Funasaki, N. *Biochim. Biophys. Acta* **1985**, *828*, 241–246.

(26) Neya, S.; Hada, S.; Funasaki, N.; Umemura, J.; Takenaka, T. *Biochim. Biophys. Acta* **1985**, *827*, 157–163.

Significance of Corrphycene Molecular Shape

Table 1. Visible Absorption Spectra of Mb-B in 0.1 M Tris at pH 7.0 and 20 °C

ligand	λ_{max} , nm (ϵ , mM ⁻¹ cm ⁻¹)				
	Ferric Derivatives				
H ₂ O	421 (93.0)	527 (6.9)	561 (6.0)	622 (7.7)	660 (3.4)
CN ⁻	420 (107.8)	543 (8.1)	680 (1.4)	752 (2.1)	
N ₃ ⁻	390* (54.3)	430 (73.3)	531 (7.8)	658 (5.7)	
F ⁻	423 (95.8)	500* (8.4)	570* (5.4)	628 (11.4)	
OCN ⁻	425 (91.8)	526 (7.5)	556 (6.7)	606 (3.7)	655 (7.2)
SCN ⁻	420 (88.5)	531 (8.5)	564 (7.5)	616 (2.7)	660 (5.4)
imidazole	417 (98.6)	538 (7.0)	667 (1.4)	751 (1.3)	
OH ⁻	427 (79.7)	590* (7.3)	622 (12.7)	(pH 9.2)	
Ferrous Derivatives					
deoxy	441 (134.0)	530 (7.4)	563 (11.1)	605 (19.5)	
O ₂ ^d	420* (71.8)	440 (90.3)	528 (8.2)	561 (10.0)	605 (13.5)
CO	414 (174.6)	505 (12.5)	525* (11.3)	695 (5.1)	

^a The O₂ saturation of the "oxyMb" is ~34% under 1 atm of air.

^b Shoulder peak with an asterisk.

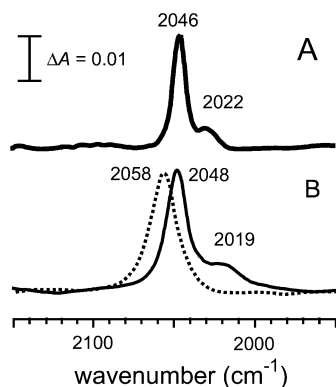


Figure 5. IR spectra of the Fe-bound azide at 20 °C: (A) Mb-B in 0.1 M Tris at pH 7.0; (B) six-coordinate azide/1-methylimidazole model complex (solid line) and five-coordinate azide complex (broken line) of ferric corrphycene B in chloroform. The sample concentration is 2–3 mM.

the single 2058-cm⁻¹ band of the five-coordinate azide complex (Figure 5). We assigned the 2049- and 2022-cm⁻¹ peaks in Mb-B to the high- and low-spin bands, respectively, from a comparison with the reported results for the native Mb (2045 cm⁻¹, high spin; 2023 cm⁻¹, low spin)^{23–25} and Mb-A (2046 cm⁻¹, high spin; 2024 cm⁻¹, low spin).¹⁴ The intensity ratio of the two bands $I_{2049}/I_{2022} = 8.8$ in Mb-B indicates predominance of the high-spin state. The protein spectrum with a large high-spin band was well reproducible in the six-coordinate model, where the high- (2048 cm⁻¹) and low-spin (2019 cm⁻¹) peaks appeared, respectively, with an intensity ratio of $I_{2048}/I_{2019} = 8.2$. It is notable that Mb-B is dominantly high-spin; the result is in contrast with the native Mb, which is mostly low-spin.²³ The difference comes from the core deformation of porphyrin into corrphycene as discussed earlier.^{14,24}

Discussion

Mb with Iron Corrphycene B. The incorporation of iron corrphycene B into apoMb is supported with a 1:1 binding stoichiometry. The IR spectral similarity between Mb-B and the six-coordinate N₃⁻/1-methylimidazole model (Figure 5) suggests ligation of the proximal histidine in Mb-B. The acid–alkaline transition in ferric Mb-B (Figure 3) further indicates that the sixth coordination site is occupied with a

water molecule. Thus, Mb-B retains the axial coordination structure identical with that in the native Mb.

Mb-B exhibits a characteristic profile as compared with Mb-A.^{13,14} For instance, the acid–alkaline transition of aquamet Mb-B (pK = 7.3) occurs at a lower pH than Mb-A (pK = 7.8).¹⁴ Thus, the migration of the functional groups from the longer to the shorter sides of the trapezoid (Figure 1) alters the acid–base property of the coordinating water molecule. It could be argued that the substituent effect is structural, rather than electronic, in nature. Because the ethoxycarbonyl (–CO₂C₂H₅) group contains hydrophilic O atoms, they could point toward the solvent sphere to direct the orientation of corrphycene A and B in the heme pocket and subsequently to modify the steric globin–corrphycene contacts. However, the different globin–corrphycene contacts in the A and B isomers, if any, would negligibly affect the iron-bound water molecule. This is because the acid–alkaline transition in Mb is known to be insensitive to the heme peripheral contacts in the protein pocket.^{27,28} It seems rather that the difference in the pK values between Mb-A and Mb-B primarily comes from the electronic effect of the ethoxycarbonyl groups. The lower pK in Mb-B indicates that the electron attraction by the side chains is stronger in corrphycene B to facilitate deprotonation of the iron-bound water molecule into hydroxide at lower pH.

Regulation of the Anionic Ligand Affinity. We stated above that the functional groups in corrphycene B more effectively behave than those in corrphycene A. This proposal is supported from the ligand-binding results. It is notable that Mb-B exhibits a 3.7-fold higher affinity for N₃⁻ than Mb-A.¹⁴ The increase in the azide affinity is small but significant because similar results are observed for CN⁻, OCN⁻, SCN⁻, and F⁻ as well. Mb-B exhibits 1.3–5.3-fold higher affinities for these anions as compared with Mb-A.¹⁴ The only exception is the bulky neutral ligand, imidazole, for which Mb-B (198 ± 14 M⁻¹) has a lower affinity than Mb-A (634 ± 57 M⁻¹).²⁹ The higher affinities of Mb-B for anionic ligands suggest that the ester groups in corrphycene B place more positive charge on the Fe atom. It is notable that Sono and Asakura reported a closely related observation for horse heart Mb reconstituted with iron porphyrins.³⁰ They found that the affinity of ferric Mb to anions increases with an increase in the number of the formyl groups of porphyrin, suggesting the significance of the electron-withdrawal effect by the heme side chain. In corrphycene A and B, on the other hand, the same number of the ethoxycarbonyl groups nonuniformly works depending on the location of the trapezoid.

Implication from Spin-Equilibrium Analysis. Stronger electron withdrawal by the side chains in corrphycene B is further supported from the spin-equilibrium analysis of the

(27) Neya, S.; Funasaki, N.; Imai, K. *Biochim. Biophys. Acta* **1989**, *996*, 226–232.

(28) Neya, S.; Funasaki, N.; Shiro, Y.; Iizuka, T.; Imai, K. *Biochim. Biophys. Acta* **1994**, *1208*, 31–37.

(29) We obtained an imidazole-binding constant of 634 ± 57 M⁻¹ to ferric Mb-A¹⁴ from the spectrophotometric titration in 0.1 M Tris at pH 7.0 and 20 °C.

(30) Sono, M.; Asakura, T. *J. Biol. Chem.* **1976**, *251*, 2664–2670.

azide complex. The six-coordinate corrphycene B without protein exhibits a more intensified low-spin IR band (Figure 5) than the corrphycene A model.¹⁴ Because the intensity ratio of the high- and low-spin IR bands $I_{\text{high spin}}/I_{\text{low spin}}$ is directly correlated with the spin-equilibrium constant [high spin]/[low spin],^{23,24,26} the larger low-spin band in corrphycene B, relative to that in the corrphycene A model,¹⁴ indicates a larger low-spin fraction in the former. The IR observation further suggests that the same is true for the iron corrphycene in the globin pocket. Mb-B in Figure 5 exhibits a more intensified low-spin IR band than Mb-A.¹⁴ The larger low spin in the corrphycene B model and Mb-B accordingly indicates that the ester groups in the bipyrrrole moiety induce a more positive charge on the iron and cause a stronger charge attraction for axial azide. The stronger axial ligand field consequently shifts the spin equilibrium to low spin. It is also notable that the iron corrphycene B and Mb-B are more low spin than corrphycene A and Mb-A. This observation indicates that the low-spin bias in Mb-B directly reflects the electron induction within the prosthetic group itself and that the globin matrix affects only slightly the heme iron. We suggested above that the lower pK of the acid–alkaline transition in Mb-B reflects the electronic effect rather than the altered globin–corrphycene interactions. The result of the spin-equilibrium analysis is consistent with the implication from the acid–alkaline transition.

Influence to the Mb Function. According to Sono and Asakura, the oxygen affinity of Mb decreases with an increase in the electron-withdrawing ability of the heme side chains.²² The decreased oxygen affinity primarily comes from the destabilization of the ferrous state due to increased positive charge on the Fe atom by the electron-inductive substituents. Mb-B ($P_{50} = 300$ mmHg; Figure 4) exhibits 8.1-fold lower oxygen affinity than Mb-A ($P_{50} = 37$ mmHg).¹³ The observation indicates that corrphycene B effectively decreases the oxygen affinity of Mb. Why does corrphycene B have more potent effects than corrphycene A in protein? The argument comes from the characteristic molecular shape of corrphycene. According to the X-ray analyses of metallocorrphycene, the metal atom is not in the middle of the coordination core but shifted toward the bipyrrrole moiety to produce the longer and shorter metal–N(pyrrole) bonds.^{1,31–33} For the ferric iron complexes, the

Fe–N(bipyrrrole) and Fe–N(dipyrroethene) distances are 2.014–2.049 and 2.049–2.079 Å, respectively.^{32,33} The inductive effect of the substituents could be transmitted more efficiently to the Fe atom through the shorter Fe–N(bipyrrrole) bonds. It is also likely that the moderately bulky ethoxycarbonyl groups on the bipyrrrole moiety of corrphycene B (Figure 1) are under steric repulsion to constrain the macrocycle. According to the X-ray analysis, nonplanar deformation of porphyrin results in a narrower coordination core.³⁴ The steric repulsion between the two ethoxycarbonyl groups in corrphycene B could deform the macrocycle and shorten further the Fe–N(bipyrrrole) bonds to enhance the difference in the Fe–N(pyrrole) bond length.

The free bases of corrphycene A and B have an identical $pK_3 = 2.4$ for the third protonation of the central N atoms. Hence, the acid–base properties of the pyrrole N atoms of the two isomers are essentially the same. However, when the iron complexes are placed in the protein pocket, corrphycene B more strongly affects the Mb function. It is notable that the oxygen affinity of Mb-B is only $1/410$ of the native Mb ($P_{50} = 0.73$ mmHg).²² The affinity is the lowest among those reported for the reconstituted Mb's with the native primary structure. This is the distinguished manifestation of the “shape effect” of corrphycene.

In summary, the present analysis demonstrates that the two pyrrole groups in corrphycene are nonequivalent. The ester side chains on the bipyrrrole part affect the central Fe to alter more seriously the properties of Mb. The site-dependent effects of the functional groups are not observed for regular porphyrin with a square tetrapyrrole. Thus, the trapezoidal molecular shape of corrphycene has a functional significance and can be utilized to regulate the function of hemoproteins.

Acknowledgment. This work was supported by a grant-in-aid for “Initiatives for Attractive Education for Graduate Schools” from Japan Society for the Promotion of Science.

IC0600679

- (31) Fowler, C. J.; Sessler, J. L.; Lynch, V. M.; Waluk, J.; Gebauer, A.; Lex, J.; Heger, A.; Zuniga-Rivero, F.; Vogel, E. *Chem.—Eur. J.* **2002**, *8*, 3485–3496.
- (32) Ohgo, Y.; Neya, S.; Ikeue, T.; Takahashi, M.; Takeda, M.; Funasaki, N.; Nakamura, M. *Inorg. Chem.* **2002**, *41*, 4627–4639.
- (33) Ohgo, Y.; Neya, S.; Funasaki, N.; Nakamura, M. *Acta Crystallogr.* **2001**, *C57*, 694–695.
- (34) Hoard, J. L. *Ann. N.Y. Acad. Sci.* **1973**, *206*, 18–31.